TECHNICAL PAPER

Static analysis of prestressed micropile-raft foundation with varying lengths resting on sandy soil

Mehdi Ebadi-Jamkhaneh[1] · Denise-Penelope N. Kontoni[2,3]

Abstract

The micropile-raft system is used in the foundation system of buildings due to the combination of the advantages of raft foundations and micropiles. In this paper, the numerical model was calibrated and validated with a field test, and then several parametric studies were performed. The overarching aim of the study is to determine the efficiency of different arrangements of micropiles and the effects of these parameters on the behavior of piled raft foundations in sandy soil. Parameters including diameter, length, and distance of micropiles from each other were considered in the analyses. Prestressed rebars have been used to increase the load-bearing capacity and prevent premature buckling under severe compressive load. Therefore, to compensate for the weak bearing capacity of the raft foundation, a micropile system equipped with prestressed rebars was considered to increase the bearing capacity of the foundation. The results revealed that using a set of micropiles with a diameter of 30 cm and a length of 10 m had the maximum efficiency among other models. Furthermore, an innovative arrangement of micropiles was proposed in which a set of micropiles with a length of 30 m was placed at the middle region of the foundation, and in the peripheral area of the foundation, several short micropiles were used.

Keywords Micropile · Load–settlement relationship · Stiffness · Soil–pile interaction · Micropile-raft foundation · Finite element analysis

Introduction

Drilling a hole in the earth and filling it with cement grout and a central reinforcing element is how micropiles (MPs) are made. A micropile (MP) distributes its weight to the soil in the bonded region between the grout and the earth largely by skin friction. The construction of MPs has greatly improved, and new construction procedures have been created. The development of strong drilling tools has made it possible to build MPs in nearly any ground condition with minimal noise and vibration. Furthermore, because of the equipment's compact size, it has been possible to underlie existing foundations even in areas where access is prohibited [1]. The main weakness of conventional MPs was that they were very prone to buckling due to compressive force, and their compressive capacity was not used properly. Therefore, by using the prestressing method, the weakness of its early buckling was addressed, and this led to an increase in its bearing capacity. Hwang et al. [1] conducted several tests on micropiled raft foundation to assess its bearing capacity; their findings revealed that the micropiles modified the failure mode of the soil and increased the bearing capacity.

The micropile raft's fundamental concept is similar to that of the piled raft, which is a composite construction made up of three parts: subsoil, raft, and piles. The pile–soil interaction, pile–soil–pile interaction, raft–soil interaction, and pile–raft interaction are all part of a complicated soil–structure interaction system. In terms of serviceability and material efficiency, the piled raft foundation system has several benefits over the pile group design. At the serviceability load, the piles will offer enough stiffness to control total and differential settlements, while the raft will provide extra capacity at the ultimate load. When studying micropile rafts,

✉ Denise-Penelope N. Kontoni
    kontoni@uop.gr; kontoni.denise@ac.eap.gr

    Mehdi Ebadi-Jamkhaneh
    m.ebadi@du.ac.ir

[1] Department of Civil Engineering, School of Engineering, Damghan University, Damghan, Iran

[2] Department of Civil Engineering, School of Engineering, University of the Peloponnese, 26334 Patras, Greece

[3] School of Science and Technology, Hellenic Open University, 26335 Patras, Greece

knowledge and expertise obtained through investigating piled rafts may be useful. To investigate the performance of piled rafts, several studies have been performed, such as Poulos and Davis [2], Bagheri et al. [3], Clancy and Randolph [4], and Poulos [5].

Several investigations have been carried out to evaluate the performance of individual micropiles and micropile groups. Full-scale load tests (e.g., Jeon and Kulhawy [6], Abd Elaziz and El Naggar [7], and Drbe and El Naggar [8]), model tests (e.g., Tsukada et al. [9]), and geotechnical centrifuge testing have all been used (Juran et al. [10]; Alnuaim et al. [11]). Different load tests on varied numbers of single and micropile group configurations were explored by Juran et al. [10]. They examined how the slenderness ratio, spacing-to-diameter ratio, and group arrangement of micropile foundation systems affected the load transfer mechanism and load-bearing capacity [10]. In addition, various micropile loading tests were performed to assess the MPs' lateral performance (e.g., Richards and Rothbauer [12]; Long et al. [13]; Shahrour and Ata [14]; and Teerawut [15]). Farghaly and Kontoni [16] investigated the mitigation of the seismic pounding between RC twin high-rise buildings with piled raft foundation considering soil–structure interaction.

The finite element analysis (FEA) is an effective technique for conducting extensive parametric analyses of piled and micropile rafts, especially when the model has been calibrated and confirmed using actual data (e.g., Rose et al. [17]). Babu et al. [18] used 2-D FEA to examine the use of MPs to improve the bearing capacity of an existing rectangular shallow foundation on sand. They discovered that placing MPs along the outside perimeter of an existing foundation at a spacing of 2 times its diameter enhanced its bearing capacity by roughly 145%. Shahrour et al. [19] used a 3D finite element study to assess the seismic performance of a single micropile and micropile groups, taking into account the number of MPs and their spacing. They discovered a favorable group effect, especially when the spacing was short ($S/D_{mp} = 3$ vs. $S/D_{mp} = 7$). Sadek and Shahrour [20] used 3D FEA to examine the behavior of inclined MPs under dynamic stress. The micropile group's spacing-to-diameter ratio (S/D_{mp}) was 5. Chaudhary [21] numerically modeled a large piled raft foundation in weak rock to control the settlement and concluded that using piles for rafts supported on weak rock is very effective in reducing settlements. Alnuaim et al. [22] studied numerically the effect of various parameters, including micropile spacing, raft thickness, and sand density on axial stiffness, differential settlement, load sharing and bending moment on the performance of micropiled raft resting on sand via 3D FE model; their results revealed that the micropiled raft system had a potential to increase the bearing pressure by 1.9 times of an isolated raft system.

Comprehensive parametric analyses of piled raft foundations in sand were also carried out using FEA. Using the 2D finite element method (FEM), Oh et al. [23] examined the impact of raft thickness and the pile spacing ratio, S/Dp, on the performance of a piled raft resting on sand and subjected to static vertical stress. The raft thickness has a considerable impact on the raft bending moment and differential settlement, but only a slight impact on the maximum settlement, according to the researchers. On a piled raft erected in medium dense sand (Dr = 45%), Baziar et al. [24] used a 1g tiny model and a 3-D finite-difference technique (FDM). The Mohr-Coulomb failure criteria were found to have excellent agreement with the results of the 1g model and numerical simulation. Furthermore, the axial stiffness of the piled raft calculated using the PDR technique agreed with the results of the 1g model. To analyze the settling of high-rise structures, Katzenbach et al. [25] used 3D FEA studies. They validated the value of numerical modeling in the design process, particularly for assessing high-rise building settlements. Ahmed et al. [26] analyzed numerically a piled raft foundation resting on clayey soil. They found that when the ratio of pile spacing to diameter exceeded 10, piles did not affect the load-bearing capacity of the foundation. Benmoussa et al. [27] investigated the bearing capacity of circular footings resting on two-layered clay soil. The results revealed that the bearing capacity related to the top layer thickness and the ratio of strength between two layers of the clayey soil. Yu et al. [28] studied the carrying capacity of cemented soil with high water content and reinforced with a group of prestressed high-strength concrete piles. The results depicted that the cemented soil strength had a large effect on the frictional capacity of the prestressed concrete pile-cemented soil interface. It should be noted that the studies conducted on prestressed micropiles are very few. Therefore, in this research, these types of micropiles were considered. Misra and Chen [29] studied the behavior of micropiles under tension and compression analytically. They proposed a function to evaluate the micropile deformation, including the effect of soil–micropile interaction and soil properties. Han and Ye [30] performed experimentally the study on a foundation resting on soft soil to investigate the load transfer mechanism when the micropiles are connected to the foundation. They suggested guidelines for designing underpinned foundations using micropiles.

The overarching aim of this research is to determine the distance and the optimal number of MPs under static loading. Also, determining the effectiveness of prestressed micropile and its effect on foundation behavior are the other goals. In other words, the effect of MP on the behavior of the raft and soil is evaluated. Based on the results, an innovative arrangement of micropiles beneath the raft foundation is proposed and analyzed under static loading.

Numerical modeling

This section presents the development and calibration of the FEM model that was used to carry out the numerical parametric study for a micropile raft installed in sand.

Validation of the numerical model

In the first step, the numerical FEM model was validated with a single MP tested at the project site [31]. This project was located in Mashhad city and had a steel structure with 22 floors [31]. The 3D FEM was established using the computer program ABAQUS [32], considering an appropriate size mesh and some elements following a sensitivity study. After ensuring the accuracy of the results and modeling method, parametric studies were performed. Figure 1 shows the final meshed model and different parts of the model.

The project has been carried out in the city of Mashhad, Iran, and at the project site of Al-Zahra Hotel with a 22-story steel structure [31]. The lower level of the foundation is − 18 m. In this regard, four different piles with lengths of 3, 6, 9, and 11 m were implemented at the project site, a loading test was performed on them, and the relevant compressive capacities were calculated. The MPs are equipped with a steel tube with an outer diameter of 76 mm and an inner diameter of 68 mm and made of steel with a yield stress of 240 MPa, as well as rebar with a nominal diameter of 30 mm and yield stress of 300 MPa. The bearing strength

of a cylindrical sample of concrete inside a tube is 30 MPa [31]. The bearing strength of 6-m MPs was about 810 kN, and of 3-m MPs was about 70 kN.

The bearing strength of micropiles was calculated based on AASHTO (2014) [33]. In the loading step, a square plate with a dimension of 200 mm × 200 mm and a thickness of 1.5 cm was placed at the centerline of the micropile, with a central hole from the inside. By placing the jack in position on the top surface of the steel plate, three displacement gauges were placed in the appropriate position, and the load test was performed.

According to the information obtained from the drilling boreholes, the bed soil consists of a compacted sandy soil consisting of fine-grained sandy soil with brown silt. The results of standard penetration tests (SPT) show several values of 10 to 20 strokes, which indicates the medium and low compaction of the desired sand layer. The physical and mechanical characteristics of this layer, on average, are presented in Table 1 [31].

The bottom surface of the soil domain is restricted just in translational directions. All rotational degrees of freedom are released. At the top level of the micropile, the force was applied in terms of displacement control. The contact and constraint in this phase are in three forms. First, the rebar contacts of the concrete are in an embedment manner using the embedded region command. Then, the surface of the steel tube is in contact with the surrounding soil. The master-slave command is used to determine the base and follower surfaces by defining the coefficient of friction between

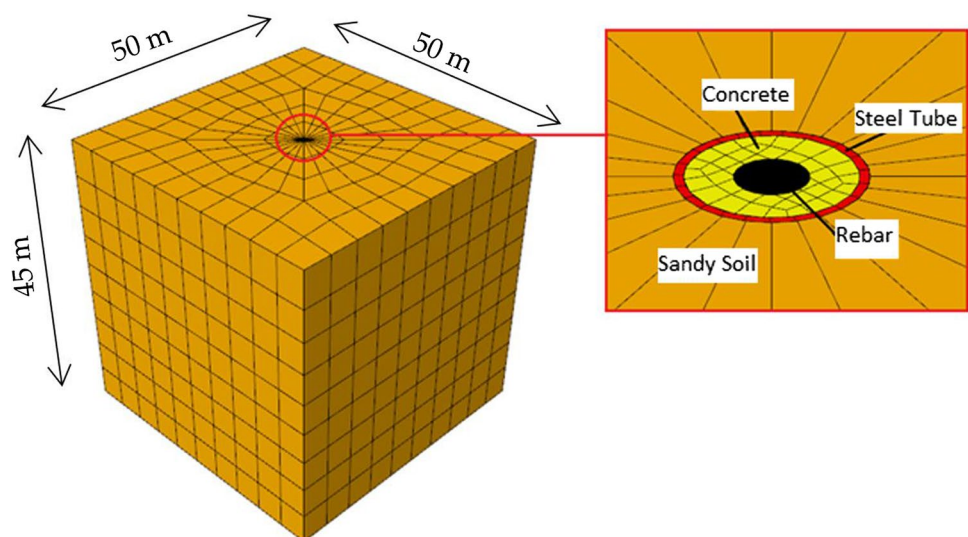Fig. 1 The numerical meshed model with different parts

Table 1 Mechanical and physical features of sandy soil

N_{SPT}	E (MPa)	Poisson's ratio	Wet density (kg/m³)	Dry density (kg/m³)	Cohesion (MPa)	Internal friction angle (°)
15	17.5	0.3	1800	1500	0.002	30
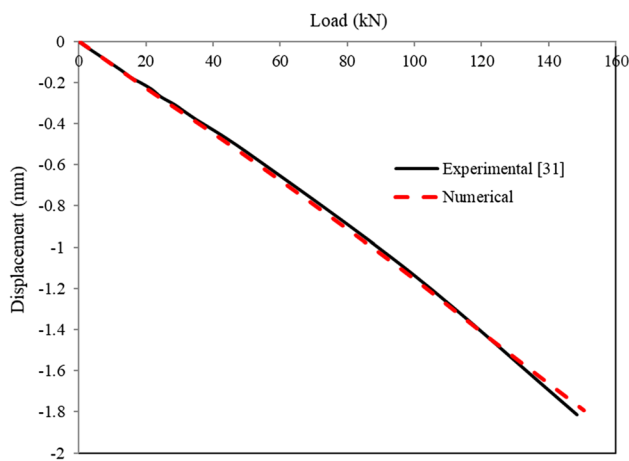
Fig. 2 Comparison of the load–displacement curve of a numerical model with the test sample

Table 2 Geometrical characteristics of micropiles (MPs)

Model no	Diameter of MP (m)	Length of MP (m)	Interval distance (m)
1	0.1	1	1
2	0.1	1	5
3	0.1	1	10
4	0.1	5	1
5	0.1	5	5
6	0.1	5	10
7	0.1	10	1
8	0.1	10	5
9	0.1	10	10
10	0.2	1	1
11	0.2	1	5
12	0.2	1	10
13	0.2	5	1
14	0.2	5	5
15	0.2	5	10
16	0.2	10	1
17	0.2	10	5
18	0.2	10	10
19	0.3	1	1
20	0.3	1	5
21	0.3	1	10
22	0.3	5	1
23	0.3	5	5
24	0.3	5	10
25	0.3	10	1
26	0.3	10	5
27	0.3	10	10

the two surfaces and the normal behavior. Finally, there is another contact surface between the inner wall of the steel tube and the confined concrete inside it, which is defined as before. Finally, after applying force to the beginning of the MP and performing nonlinear statics, the load-displacement curve of the numerical FE model is extracted and compared with the experimental sample, which is shown in Fig. 2. Figure 2 shows a comparison of the experimental and numerical load-displacement curve in the elastic region. For loading beyond the elastic range, unfortunately, there was no experimental data to be compared with FE model in the plastic region. However, the FE model can be considered for capturing the nonlinearity features of the MP models.

Definition of the numerical models

To investigate the effect of the parameters of length, diameter, and distance of MPs, a range of 1–10 m was considered for the length and distance between MPs and a range of 100–300 mm for the diameter of MPs. Details of the models are given in Table 2. A total of 27 models were simulated for analysis. It should also be noted that in FE models with a distance of 1 m, the number of MPs is equal to 225. In models with a distance of 5 m, this is equal to 16, and in models with a distance of 10 m is equal to 4.

The plan of the foundation has dimensions of 15 ×15 m with a thickness of 1 m. The raft thickness of 1 m is adequate for the model; however, the thickness of the raft was not the main concern of this study. Also, sandy soil characteristics have been used from the validation case. If a 10-story steel structure with a bracing system is placed on the foundation, the load due to the total weight of this structure will be equal to 47.5 MN. For instance, model 1 is shown in Fig. 3.

Since the rebar is embedded in concrete, the prestressing force with just 10% of the total bearing strength of MP

was applied using the bolt load command. In ABAQUS, the structure must reach a state of equilibrium without any external force applied (or only with dead loads) before active loading by an initial static analysis step. It should be noted that this is only possible in cases where the rebar is defined using the rebar layer technique.

It is usually assumed in MP design that the load is transferred to the ground through soil-slurry friction, and the participation of the bearing capacity related to the MP's tip is excluded. The amount of allowable load for the length of the geotechnical bond is calculated by the allowable stress method according to Eq. 1.

$$P_{G-all} = \frac{\alpha_b}{FS} \times \pi \times D_b \times L_b \qquad (1)$$

In this regard, $P_{G\text{-all}}$ is the geotechnical bearing capacity of the MP wall, L_b is the length of the MP, D_b is the diameter of the MP, FS is the safety factor (FS = 2.0), and α_b is the resistance of the connection between the MP and the
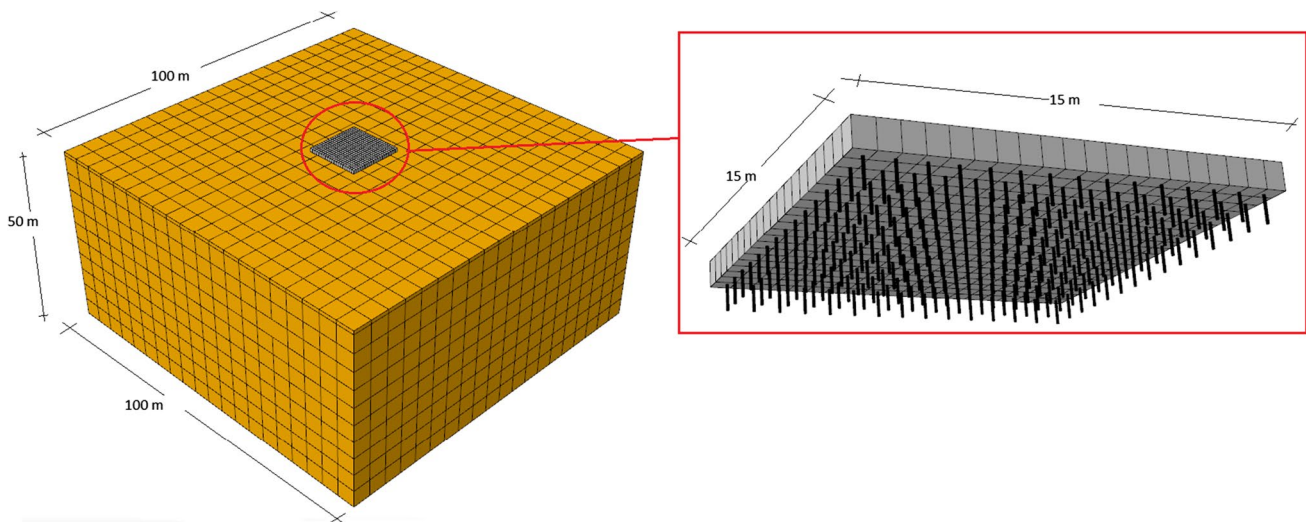
Fig. 3 Meshed model of FE model 1

Table 3 Specifications of allowable loads of MPs (Unit: kN)

No	$P_{G\text{-all}}$	$P_{C\text{-all}}$	$P_{T\text{-all}}$
1–3	15.7	100.292	46.63
4–6	78.5	100.292	46.63
7–9	157	100.292	46.63
10–12	31.4	421.451	88.1
13–15	157	421.451	88.1
16–18	314	421.451	88.1
19–21	47.1	962.41	129.525
22–24	235.5	962.41	129.525
25–27	471	962.41	129.525

surrounding soil. The value of the bond strength is equal to 100 kPa following the FHWA Report [34], which in Table 3 of this Code has been adopted.

Based on the compatibility of the strain between the tube and the reinforcing rebar, the yield stress of the micropile (F_y) is equal to at least two values of the yield stress of the reinforcing rebar (F_{yb}) and the yield stress of the steel tube (F_{yc}). Permissible tensile and compressive loads of MPs are also obtained using the following equations [34].

$$P_{T-all} = 0.55F_y \times (A_b + A_c) \tag{2}$$

$$F_a = \frac{F_y}{FS}, FS = 2.0 \tag{3}$$

$$P_{C-all} = 0.4f_{cgr} \times A_{gr} + 0.47F_y(A_b + A_c)$$

Finally, the final bearing capacity of the micropile is calculated from Eq. 4 [34].

$$P_{total} = \min\left(P_{G-all}, P_{C-all}, P_{T-all}\right) \tag{4}$$

where A_b is the cross-sectional area of the rebar, A_c is the cross-sectional area of the steel tube, F_a is the allowable stress (allowable strength), f_{cgr} is the compressive strength of the grout, A_{gr} is the cross-sectional area of the grout. P_{G-all} is the allowable load of the pile wall, P_{C-all} is the allowable compressive load, P_{T-all} is the allowable tensile load, and P_{total} is the final allowable load of the micropile. Table 3 shows the values of allowable loads.

Numerical modeling features

Soil–structure interaction plays an important role in the behavior of the structure under static or dynamic loading. It influences the behavior of soil, as well as the response of piles under loading. The analysis is highly essential for predicting a more accurate structural behavior to improve the safety of structures under extreme loading conditions. The soil–pile system behavior is predominantly nonlinear, and this makes the problem complicated.

The soil and MPs were modeled using 3D 10-node tetrahedral elements, while the raft was modeled using 6-node triangular plate elements. The total number of elements of the model was 178,250, with an average element size of 100 mm. A large number of small-size elements assured high accuracy of the results at locations where nonlinear behavior was anticipated (e.g., raft base, micropile base, and micropile circumference). The load was applied as a concentrated load on a rigid dummy plate at the center of the raft. The behavior of the raft and MPs was simulated considering a linear elastic model considering the mechanical properties of concrete (elastic modulus, E_c, and Poisson's ratio, υ_c). The behavior of the sand was simulated using a linear

elastic–perfectly plastic constitutive model and the Mohr-Coulomb failure criterion. The peak friction angle (φ) for sand was evaluated as 30^0 from direct shear tests conducted with different vertical stress values. To adequately simulate the actual behavior of sand in which the stiffness of the sand depends on the confining stress, a function is implemented in ABAQUS [32], which allows simulating the increases in the modulus of elasticity (E_s) with depth:

$$E(z) = E_0 + (z_{ref} - z)E_{inc} \quad z < z_{ref} \quad (5)$$

where $E(z)$ = modulus of elasticity (kPa); E_0 = initial modulus of elasticity (kPa); z_{ref} = the reference depth (m); z = depth of interest (m); and E_{inc} = the rate of the increase in modulus of elasticity (kPa/m).

The finite sliding tracking approach implies that the relative motion between the contacted surfaces is tracked all the time. Thereby, the area and pressure of the contact are calculated according to the deformed shape of the model. The contact of these two surfaces is of two components; a component normal to the surface and one tangential to the surfaces. The normal behavior between the micropile and the ground is modeled using "Hard contact". Hard contact is applied as long as the clearance or the distance between the surfaces is zero, which gives a positive contact pressure value. If the clearance is higher than zero, the contact pressure is a negative value, and the two surfaces are no longer in contact. Tangential component: is defined as the behavior along the ground interface that involves the relative sliding between surfaces that would transmit shear forces across the interface. Penalty type with the Coulomb friction model is selected to simulate the shear behavior. The coulomb friction model implies that no load transfer occurs unless the surface traction reaches the critical value of the shear stress. Tie constraint implies that each node in the slave master, micropile, has the same displacement values of the master surface, i.e., the ground. Tie also connects the MPs' parts to ensure continuity.

Results

These results include foundation settlement and soil-bearing capacity. Also, the distribution of plastic strains in the soil is shown. In the first step, the foundation was modeled and analyzed under the applied gravity load without the presence of MPs. The force-displacement diagram of the model without MPs is shown in Fig. 4. According to this figure, it is clear that the structure and foundation will settle on the soil at a rate of 88.6 cm.

Since the amount of load is 47.5 MN, so all this force must be borne by the soil, which is not able to withstand it, and the stress applied to the soil is almost twice its allowable stress.

## MP models with a diameter of 10 cm

Now, MPs with a diameter of 10 cm and a length of 1 m, which are located at a distance of 1 m from each other, are used to increase the bearing capacity and reduce deflection. In Fig. 5, the comparison between load–displacement curves of FE models is represented. In the case of using MPs with a diameter of 10 cm and placing them at a distance of 1 m from each other, the initial stiffness of the system has increased significantly due to the presence of 225 MPs, which has reduced the settlement of the structure by 87%. Figure 6 shows the equivalent plastic strain distribution under the foundation. The formulation of the flow rule and equivalent plastic strain were implemented in ABAQUS [35]. According to Fig. 6, it is clear that in model no. 3, many plastic areas have formed around the foundation plan and the bottom part of the micropiles.

In this group of MPs, from the total load, the amount of approximately 3.5 MN can be tolerated and transferred to the soil by the wall resistance. Therefore, the rest of the applied load (47.5–3.5 = 44 MN) should be borne by the soil, and the amount of applied stress is about 0.18 MPa.

As can be seen from Fig. 5, with increasing the distance between the MPs, the axial stiffness of the system decreased, which consequently increased the settlement of the system (No. 2 and 3). The allowable settlement for a raft foundation is equal to seven centimeters, which exceeds the allowable value if the arrangements of the two models No. 2 and 3 are used. If No. 2 and 3 are used, the rupture will be of the wall resistance type. Because in model number 2, only 250 kN, and in model No. 3, only 100 kN are transmitted by their wall.

In the group of MPs with a length of 5 m, the total strength of the wall will be approximately equal to 17.5 MN, which will bear 37% of the total load. Therefore, the remaining load (30 MN) must be tolerated by the soil, and the average stress applied to the soil will be equal to 0.13 MPa. Model No. 4 is the same as No. 1 by increasing the length of the micropile from 1 to 5 m. As the length increases, as predicted, the settlement of the system decreases due to the increase of the peripheral environment and, consequently, the increase of the frictional resistance. At the same time, the stiffness increases by 23% compared to model No. 1. In Fig. 7, the plastic strain distribution is shown for model No. 4.

In the case of using MPs with a diameter of 10 cm, a length of 10 m, and a distance of 1 m, the displacement has been significantly reduced compared to model No. 1. Because in the models with a length of 10 m, the compressive strength of each micropile is approximately 100 kN, and
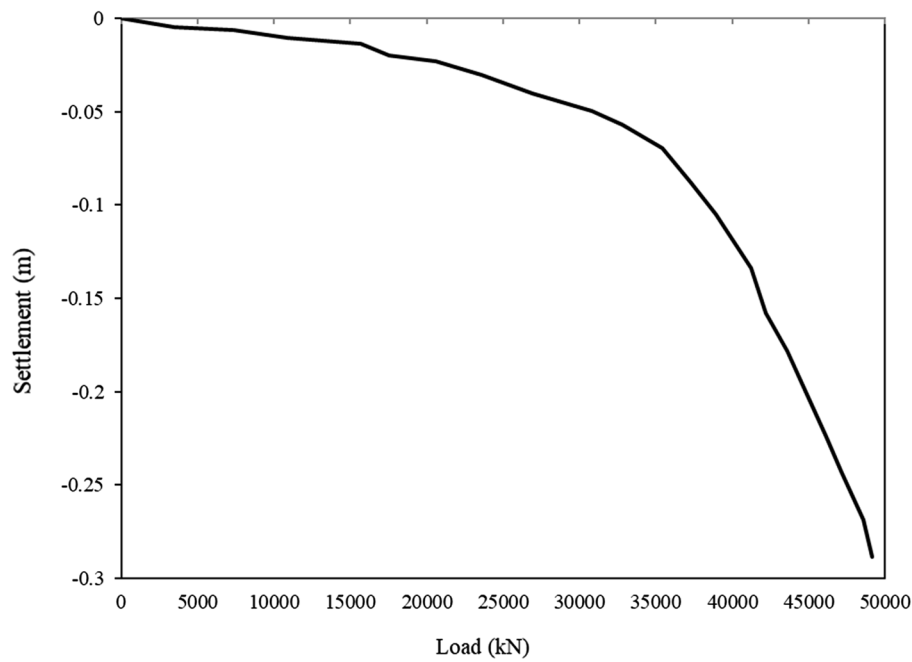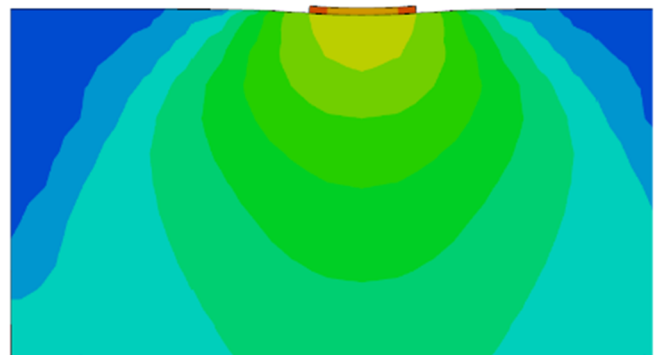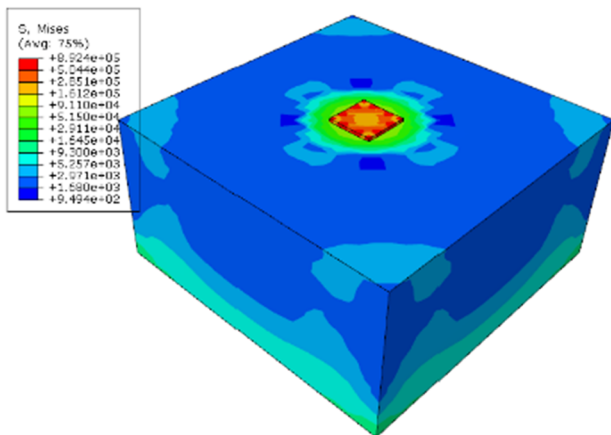
Fig. 4 Load–displacement relationship and stress contour: **a** Load–displacement curve; **b** distribution of stress on the soil

their wall resistance is 157 kN. Therefore, it is expected that rupture will occur due to the compressive force applied to the MPs. In other words, if ordinary rebars are used in them, the rupture of the MPs will be of the buckling mode, and the bearing capacity will decrease. In other words, from the total applied load, only 22.5 MN are borne by the MPs, which is only 47% of the total applied gravity load. However, because the prestressing operation by the prestressing method prevents buckling under the compressive force applied to the MPs, therefore, the rupture in the compressive mode of the MPs has been prevented. However, the compressive force that can be tolerated by MPs is less than the wall resistance, so the rupture changes from the buckling state of them to

the yield of MPs due to reaching its final limit. However, the residual stress for the soil is about 0.11 MPa. In Fig. 8, the stress and equivalent plastic strain distributions are shown for model No. 5.

As can be seen, in the category of MPs with a diameter of 10 cm, the lowest and highest settlements are related to them with a length of 10 m and a distance of 1 m, and MPs with a length of 1 m and a distance of 10 m, respectively. In this group of MPs with a length of 10 m, grout with higher compressive strength can be used to increase the bearing capacity and reduce deflection. If a slurry with higher compressive strength is used, the settlement can be reduced and placed within the allowable range. In
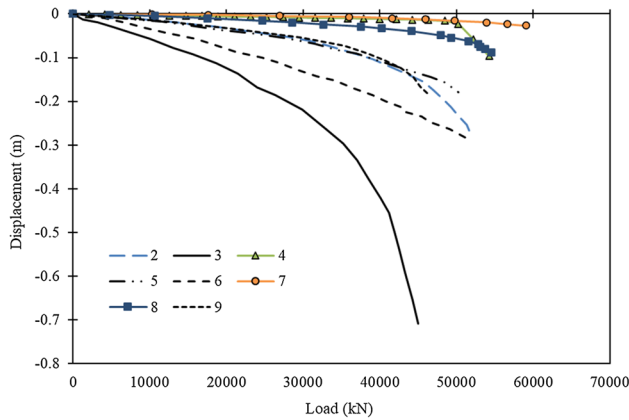
Fig. 5 Load–displacement curves of MPs with a diameter of 10 cm

this category, only MPs with a length of 10 m and a distance of 1 m were able to control the structural settlement. It should be noted that the prestressed force was 40 kN. In other words, from the total amount of load 47.5 MN, 9 MN in 1-m MPs, 6.4 MN in the 5-m length of MPs, and 1.6 MN in 10-m MPs are reduced. In the best situation with a distance of 1 m and a length of 10 m, the applied load is 30.5 MN, and the stress applied to the soil is about 0.73 kg/cm^2 (i.e., about 0.07 MPa). Therefore, by combining the two methods of prestressed rebar and increasing the compressive strength of the grout, it is possible to control the structural settlements. In this category, only model No. 7 was able to control the settlement.

MP models with a diameter of 20 cm

In this section, the behavior of MPs with a diameter of 20 cm is investigated. Figure 9 shows the load settlement for this group from model No. 10 to model No. 18.

First, Model No. 10, with a length of 1 m and a distance of 1 m, is examined. In this group, a prestressed force of 80 kN has been applied. In total, approximately 18 MN are returned by this force. This value is valid for MPs with a distance of 1 m. According to Fig. 9, the maximum displacement of the 10-story structure located on this foundation is equal to 4.77 cm by using MPs with a distance of 1 m from each other. So, 7.06 MN is tolerated by the tube wall, and the rest of the load is sustained by the soil. Therefore, the applied stress to the soil is expected to be about 1 kg/cm^2 (i.e., about 0.1 MPa).

By increasing the distance between the MPs to 5 m, the number of MPs reaches 16. However, this number can only reduce the total load by about 1.3 MN through the tensile force alone. The wall can also carry loads up to 500 kN, and the stress in the soil is approximately 2 kg/cm^2. According to the applied load of the 10-story structure, due to the use of MPs with a diameter of 20 cm and a length of 1 m with a distance of 1 m, the settlement is equal to 4.77 cm. If a distance of 5 and 10 m is used, the settlement is equal to 10.37 cm and 26.12 cm, respectively. So, the case with a distance of 10 m is outside the allowable range of structural stability. Also, the settlement for the model with an interval distance of 10 m was more than the allowed settlement in the FHWA [34] regulations. In model No. 12, there are only four MPs, which means that they cannot play a role in structural control.
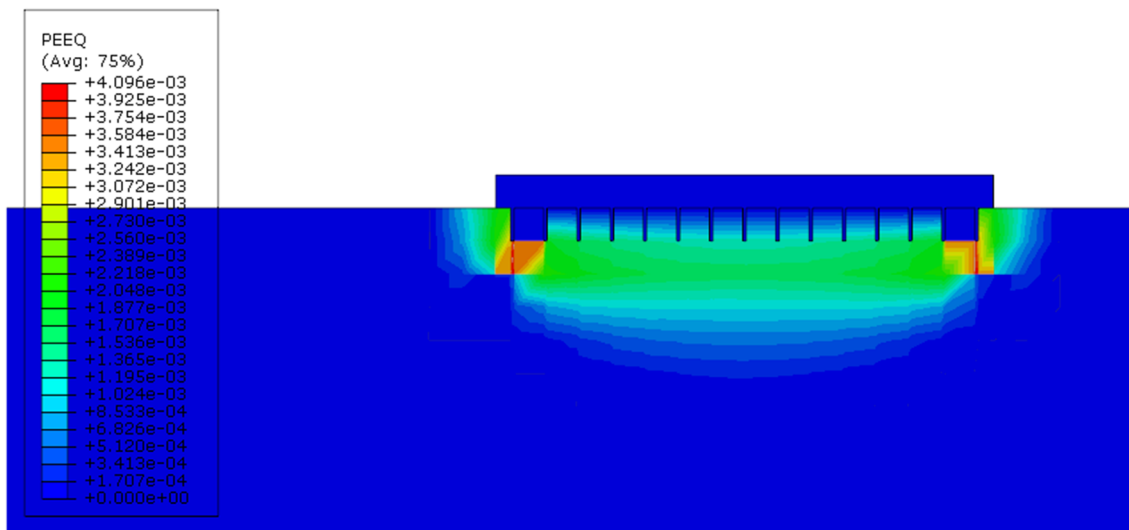

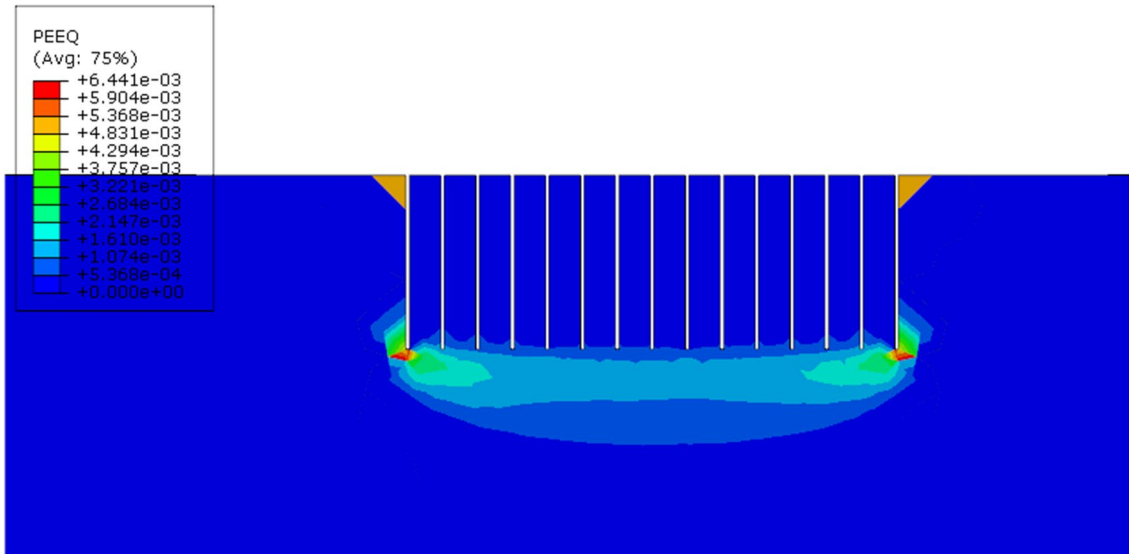**Fig. 6** Plastic strain contour on the soil

Fig. 7 Distribution of plastic strain in model No. 4

The force-displacement relationship of model No. 13 in Fig. 9 shows an 18% decrease in settlement compared to the same model with a length of 1 m (model No. 10). In all models of this category (models No. 13, 14, and 15), the failure mode is the type of wall resistance. In model No. 13, with the participation of 225 MPs, the friction resistance of the tube to the surrounding soil is approximately 35 MN, with a prestressed force of 18 MN, and practically no settlement is expected from the structure. This system is recommended for structures of historical importance that should not have any settlements. In model No. 14, only 2.5 MN of the total load is borne by the wall and 1.3 MN by the previous prestressed force. Therefore, the rest of the applied stress force is approximately 1.9 kg/cm^2, which causes a 10 cm settlement.

In the following, models with a length of 10 m and a diameter of 20 cm with a prestressing force of 80 kN are examined. In model No. 16, only the wall strength is so high that it can withstand a force of 70 MN. Therefore, in this system, there is no need to apply prestressing force. However, the force, which will total 18 MN, is used. As expected from Fig. 9, very little settlement is created in the system. The displacement equal to 1.7 cm is caused by the applied loads. In model No. 17, the total wall strength is only 5 MN, which is 10% of the total applied force. The total prestressing force is equal to 1.3 MN, which will remain at 41.2 MN, which imposes stress equivalent to 1.8 kg/cm^2 on the soil. In this model, the overall settlement is equal to 18 cm. In model No. 18, there are only four MPs with a length of 10 m, which have a friction strength of 1.25 MN and a prestressed strength of 320 kN. But this amount of force cannot prevent excessive stress applied to

the soil, which causes the system to settle approximately 47 cm.

MP models with a diameter of 30 cm

In this category, a prestressed force of 130 kN is applied to each micropile, which in models with a distance of 1 m, a total force of 29.25 MN is created. Model No. 19 includes MPs with a diameter of 30 cm and a length of 1 m with a distance of 1 m from each other. The shear strength of the steel wall is equal to 1.06 MN, which in total is 39.85 MN of shear strength to withstand the weight of the whole structure. The rest of the load applies a stress equivalent to 0.34 kg/cm^2 to the soil. In model No. 22, the micropile with a diameter of 30 cm, a length of 5 m, and a distance of 1 m from each other are subjected to gravity loading. The presence of 225 MPs creates a strong shear force of 53 MN, which is responsible for the settlement and stress of the soil. Therefore, in this model, there is no need for the presence of a prestressing force. However, this force has been applied. The total prestressing strength in this model is equal to 29.25 MN. According to Fig. 10, a small settlement has been created due to the presence of the structure on the soil, which is due to the presence of a large number of MPs.

In model No. 25, MPs with a length of 10 m were used, which were placed at a distance of 1 m from each other. In this model, there are 29.25 MN of force due to prestressing and 106 MN of force due to wall resistance. For this reason, very little settlement is observed in Fig. 10.

According to the results, the distance of 1 m of MPs from each other and the length of 5 and 10 m with a diameter of 20 and 30 cm have shown the best performance
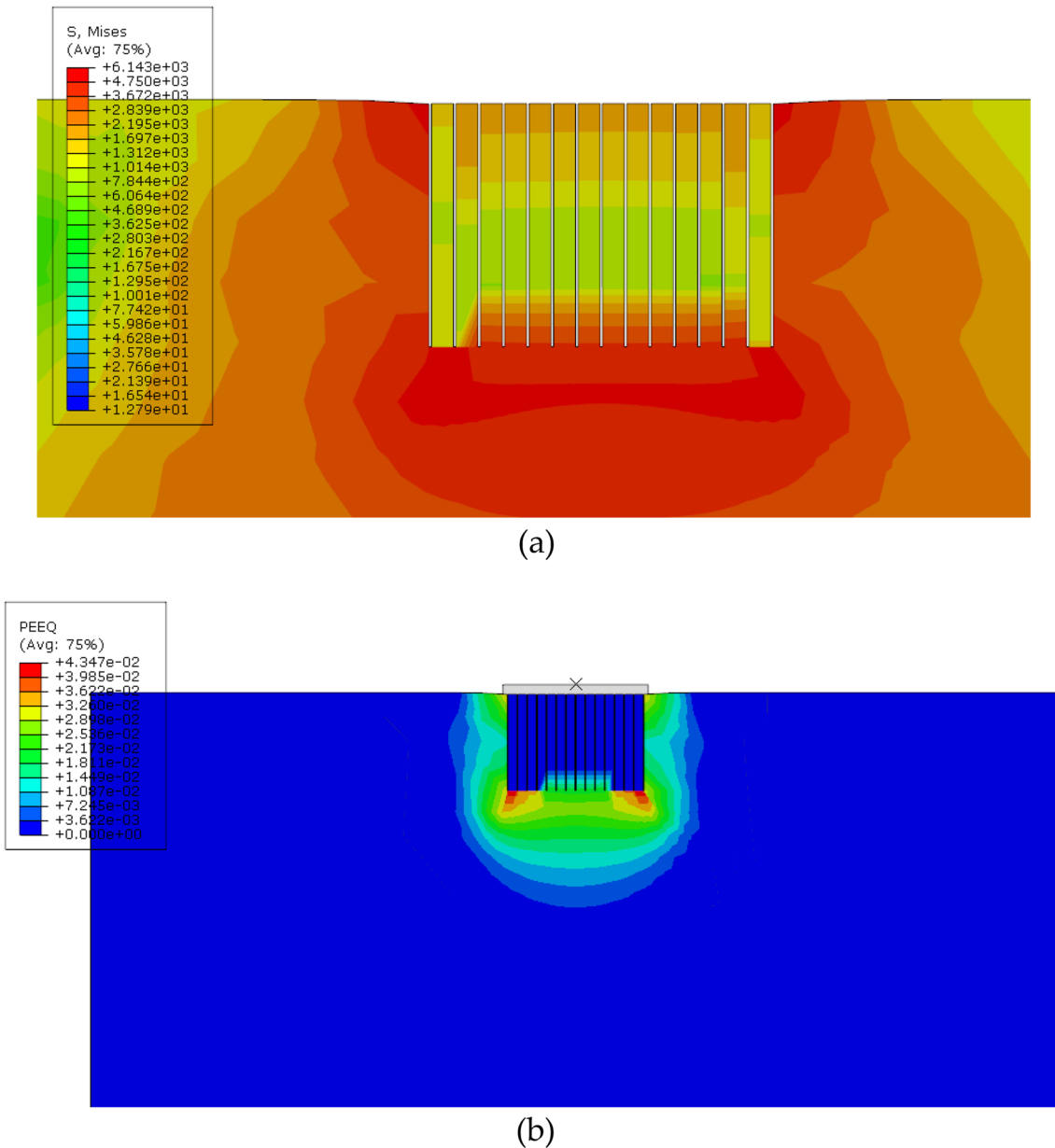
(a)

(b)

Fig. 8 Stress and plastic strain distributions for model No. 5: **a** stress contour; **b** plastic strain

among other models. In other words, the effect of increasing the length on the bearing capacity and decreasing the displacement is more and better than increasing the diameter of the micropile. Table 4 summarizes the results of the models in increasing the bearing capacity and reducing the settlement.

Figure 11a shows the effect of increasing the diameter by keeping the length and distance constant as a percentage of efficiency (models No. 1, 10, and 19 are compared in Fig. 11a). Also, Fig. 11b shows the effect of increasing the length of the micropile on the efficiency of the system, assuming that the distance and diameter remain constant.

Proposed a configuration of MPs

From the results and figures in previous sections, it can be seen that in the MPs with a length of 1 m, the middle part of the concrete slab of the foundation has the most settlement. For this purpose, it is recommended to use MPs with a diameter of 30 cm and a length of 10 m, and a distance of 1 m in the middle part and MPs with a length of 1 m, a diameter of 10 cm, and a distance of 1 m in the side parts. Figure 12 shows a schematic of this proposed configuration. The proposed configuration does not claim to be the optimum one, but among other tested models,
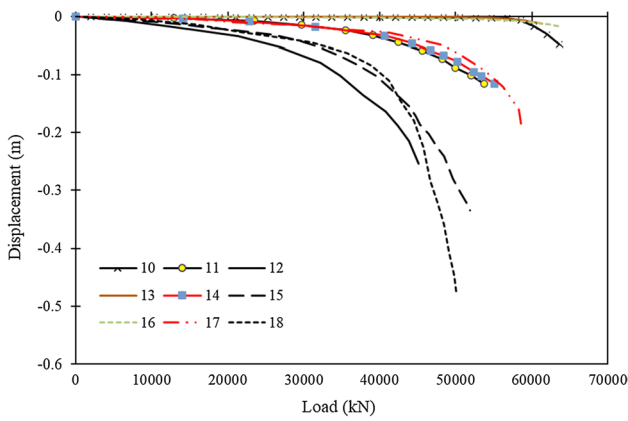
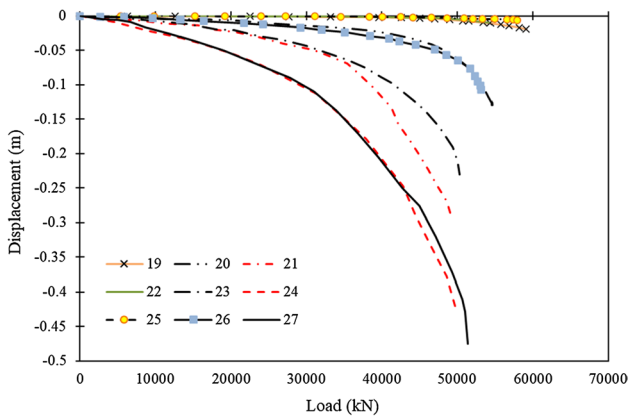**Fig. 9** Load–displacement relationship for MPs with a diameter of 20 cm

Fig. 10 Load–displacement relationship for MPs with a diameter of 30 cm

Table 4 Synopsis of the numerical models' results

Model no	Settlement (cm)*	Bearing capacity (kN)	Efficiency ratio**
1	10.37	52,173	1.10
2	27.23	51,032	1.08
3	70.88	49,723	1.05
4	9.61	59,407	1.25
5	17.84	53,075	1.12
6	28.42	50,207	1.06
7	**2.66**	60,233	1.27
8	8.78	56,192	1.19
9	18.73	51,713	1.09
10	**4.77**	56,293	1.19
11	11.54	53,102	1.12
12	25.31	50,317	1.06
13	**1.22**	61,008	1.29
14	11.51	55,281	1.17
15	33.40	51,032	1.08
16	**1.67**	62,373	1.32
17	19.64	58,066	1.22
18	47.75	54,912	1.16
19	**1.96**	57,815	1.22
20	14.13	54,219	1.14
21	28.85	51,093	1.08
22	**0.97**	63,135	1.33
23	23.10	57,557	1.21
24	42.94	53,461	1.13
25	**0.60**	63,565	1.34
26	10.67	59,437	1.26
27	47.47	55,920	1.18

Bold values indicate models with settlement less than the allowable settlement of 7 cm

*The allowable settlement is 7 cm

**Efficiency ratio is the ratio of bearing capacity to total structure's weight load

it was chosen as the best configuration due to its proper performance.

In this case, a prestressed force of 40 kN was proposed for piles with a diameter of 10 cm and a length of 1 m around the foundation and a prestressed force of 130 kN for middle MPs with a diameter of 30 cm and a length of 10 m. The prestressed force of the whole is 11.25 MN. Also, the shear strength of the wall for the middle MPs is equal to 11.77 MN and 3.14 MN for the MPs away from the middle section of the foundation, which creates a total of approximately 15 MN of the shear strength of the wall. These forces produce a total of 26.25 MN of resistant force, and the rest of the force is tolerated by the soil. The average stress in the soil is equal to 0.948 kg/cm^2. Due to the presence of prestressed rebars, the issue of premature buckling and reduction of bearing capacity has also been tackled. Figure 13 of the proposed force-displacement curve shows the success of this method in reducing structural settlement.

The use of MPs causes the subsoil layers to be sewn, and also, by providing sufficient constraint at the end of the MPs and prestressing the rebars in them, a large force is applied to keep the concrete slab towards the soil and consequently increase the capacity. Arrangements can improve the bearing capacity of foundations. In this method, due to the fact that the MPs are under tension, there is no concern about their buckling. Their tension state and the presence of load from the concrete slab allow large amounts of load to be applied to the soil.
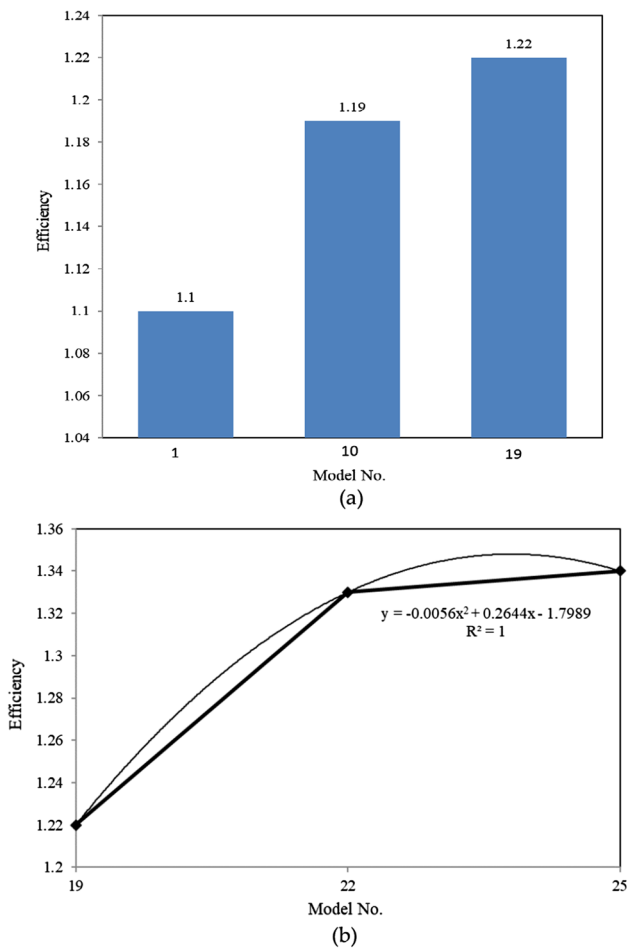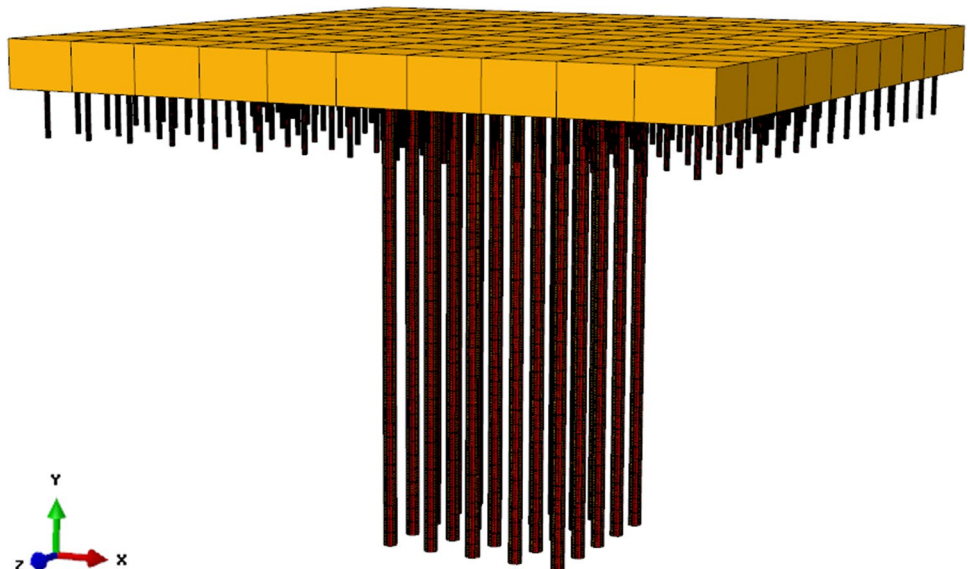
Fig. 11 Effect of increasing in diameter and length of MPs on efficiency: **a** effect of increasing in diameter of MP; **b** effect of increasing in length of MP

Fig. 12 The proposed configuration of MPs

Conclusions

Twenty-seven finite element analyses were carried out to investigate the performance of the micropile rafts installed in sand using a 3D finite element model that was calibrated and verified using experimental results. The effect of different factors on the MP's tolerable bearing pressure, axial stiffness, differential settlement, load sharing, and micropile skin friction was examined. The factors that were considered in the analysis are micropile spacing, diameter, and length. Several conclusions can be drawn from the numerical program:

1. In all models, by increasing the diameter and length of MP, the efficiency of the system increased. The effect of increasing the length on the bearing capacity and decreasing the displacement is more and better than increasing the diameter of the micropile.

2. As can be seen from the preliminary results, the proposed method (different configuration) can strengthen the foundation (without any damage) and increase its capacity. It has also been shown that this increase is mainly due to superstructure pressure, and MPs cannot be very effective in tolerating the pressure, and the increase in capacity is applied to the concrete slab by tensile loading applied by MPs.

3. In high-rise buildings, with more than 15 floors resting on sandy soil, due to the high weight of the structure, the distribution of MPs under the foundation becomes denser, and the distances between them are reduced. Hence, the bearing capacity of MPs reduces and is not cost-effective.

4. The effect of length in reducing the settlement is greater than the diameter of the micropile. Also, MPs with a
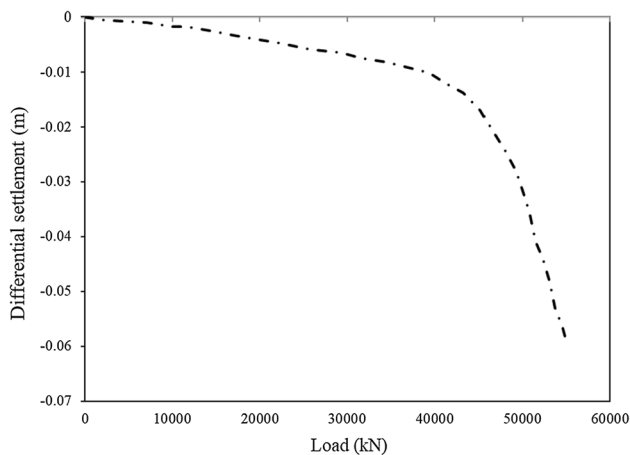
Fig. 13 The load–settlement curve of the proposed configuration of MPs

1-m length do not play a role in bearing capacity and reduced settling. Therefore, the proposed combination plan is a good option to achieve the desired goal.

5. A combination of various lengths of micropiles under the raft foundation is proposed. By using this technique, the average effective stress of the soil is around 0.95 kg/cm^2.

6. Based on the results, using different layers and thicknesses of soil can be a decent challenge in the study of the behavior of combined micropile-raft foundation.

Declarations

Conflict of interest The authors declare that there are no conflicts of interest.

Ethical approval This article does not contain any studies with human participants or animals performed by any of the authors.

Informed consent For this type of study formal consent is not required.

References

1. Hwang TH, Kim KH, Shin JH (2017) Effective installation of micropiles to enhance bearing capacity of micropiled raft. Soils Found 57(1):36–49. https://doi.org/10.1016/j.sandf.2017.01.003

2. Poulos HG, Davis EH (1974) Elastic solutions for soil and rock mechanics. Wiley, New York

3. Bagheri M, Jamkhaneh ME, Samali B (2018) Effect of seismic soil–pile–structure interaction on mid-and high-rise steel buildings resting on a group of pile foundations. Int J Geomech 18(9):04018103. https://doi.org/10.1061/(ASCE)GM.1943-5622.0001222

4. Clancy P, Randolph M (1996) Simple design tools for piled raft foundations. Geotechnique 46(2):313–328. https://doi.org/10.1680/geot.1996.46.2.313

5. Poulos H (2001) Piled raft foundations: design and applications. Geotechnique 51(2):95–113. https://doi.org/10.1680/geot.2001.51.2.95

6. Jeon SS, Kulhawy FH (2001) Evaluation of axial compression behaviour of micropiles. In: Proceedings of a specialty conference: foundations and ground improvement (GSP 113), Virginia, USA, ASCE, pp 460–471

7. Abd Elaziz AY, El Naggar MH (2014) Geotechnical capacity of hollow-bar micropiles in cohesive soils. Can Geotech J 51(10):1123–1138. https://doi.org/10.1139/cgj-2013-0408

8. Drbe OF, El Naggar MH (2014) Axial monotonic and cyclic compression behaviour of hollow-bar micropiles. Can Geotech J 52(4):426–441. https://doi.org/10.1139/cgj-2014-0052

9. Tsukada Y, Miura K, Tsubokawa Y, Otani Y, You G (2006) Mechanism of bearing capacity of spread footings reinforced with micropiles. Soils Found 46(3):367–376. https://doi.org/10.3208/sandf.46.367

10. Juran I, Benslimane A, Hanna S (2001) Engineering analysis of dynamic behaviour of micropile systems. Transp Res Rec J Transp Res Board 1772(1):91–106. https://doi.org/10.3141/1772-11

11. Alnuaim AM, El Naggar H, El Naggar MH (2015) Performance of micropiled raft in sand subjected to vertical concentrated load: centrifuge modeling. Can Geotech J 52(1):33–45. https://doi.org/10.1139/cgj-2014-0001

12. Richards TD, Rothbauer MJ (2004) Lateral loads on pin piles (micropiles). In: Proceedings of sessions of the GeoSupport conference: innovation and cooperation in the geo-industry. ASCE, Orlando, pp 158–174. Doi: https://doi.org/10.1061/40713(2004)7

13. Long J, Maniaci M, Menezes G, Ball R (2004) Results of lateral load tests on micropiles. In: Proceedings of sessions of the GeoSupport conference: innovation and cooperation in the geo-industry. ASCE, Orlando, pp 122–133. https://doi.org/10.1061/40713(2004)4

14. Shahrour I, Ata N (2002) Analysis of the consolidation of laterally loaded micropiles. Ground Improv 6(1):39–46. https://doi.org/10.1680/grim.2002.6.1.39

15. Teerawut J (2002) Effect of diameter on the behaviour of laterally loaded piles in weakly cemented sand. Ph.d dissertation. University of California, San Diego. https://books.google.com/books?id=rxpEAQAAIAAJ

16. Farghaly AA, Kontoni D-PN (2022) Mitigation of seismic pounding between RC twin high-rise buildings with piled raft foundation considering SSI. Earthq Struct 22(6):625–635. https://doi.org/10.12989/EAS.2022.22.6.625

17. Rose A, Taylor R, El Naggar M (2013) Numerical modelling of perimeter pile groups in clay. Can Geotech J 50(3):250–258. https://doi.org/10.1139/cgj-2012-0194

18. Babu SG, Murthy SB, Murthy D, Nataraj M (2004) Bearing capacity improvement using micropiles a case study. In: The GeoSupport conference: drilled shafts, micropiling, deep mixing,

remedial methods, and specialty foundation systems. American Society of Civil Engineers, Orlando, pp 692–699. https://doi.org/10.1061/40713(2004)14

19. Shahrour I, Sadek M, Ousta R (2001) Seismic behaviour of micropiles: used as foundation support elements: three-dimensional finite element analysis. Transp Res Rec J Transp Res Board 1772(1):84–90. https://doi.org/10.3141/1772-10

20. Sadek M, Shahrour I (2004) Three-dimensional finite element analysis of the seismic behaviour of inclined micropiles. Soil Dyn Earthq Eng 24(6):473–485. https://doi.org/10.1016/j.soildyn.2004.02.002

21. Chaudhary MTA (2007) FEM modelling of a large piled raft for settlement control in weak rock. Eng Struct 29(11):2901–2907. https://doi.org/10.1016/j.engstruct.2007.02.001

22. Alnuaim AM, El Naggar MH, El Naggar H (2007) Numerical investigation of the performance of micropiled rafts in sand. Comput Geotech 77:91–105. https://doi.org/10.1016/j.compgeo.2016.04.002

23. Oh EY-N, Huang M, Surarak C, Adamec R, Balasurbamaniam A (2008) Finite element modelling for piled raft foundation in sand. In: Proceedings of the eleventh East Asia–Pacific conference on structural engineering and construction (EASEC-11) building a sustainable environment, November 19–21, Taipei, Taiwan

24. Baziar M, Ghorbani A, Katzenbach R (2009) Small-scale model test and three-dimensional analysis of pile-raft foundation on medium-dense sand. Int J Civ Eng 7(3):170–175

25. Katzenbach R, Schmitt A, Turek J (2005) Assessing settlement of high and rise structures by 3D simulations. Comput Aided Civ Infrastruct Eng 20(3):221–229. https://doi.org/10.1111/j.1467-8667.2005.00389.x

26. Ahmed D, Bttaib SNL, Ayadat T, Hasan A (2022) Numerical analysis of the carrying capacity of a piled raft foundation in soft clayey soils. Civil Eng J 8(4):622–636. https://doi.org/10.28991/CEJ-2022-08-04-01

27. Benmoussa S, Benmebarek S, Benmebarek N (2021) Bearing capacity factor of circular footings on two-layered clay soils. Civ Eng J 7(5):775–785. https://doi.org/10.28991/cej-2021-03091689

28. Yu JL, Zhou JJ, Gong XN, Zhang RH (2021) Shaft capacity of prestressed high strength concrete (PHC) pile-cemented soil column embedded in clayey soil. Soils Found 61(4):1086–1098. https://doi.org/10.1016/j.sandf.2021.05.006

29. Misra A, Chen CH (2004) Analytical solution for micropile design under tension and compression. Geotech Geol Eng 22(2):199–225. https://doi.org/10.1023/B:GEGE.0000018356.85647.79

30. Han J, Ye SL (2006) A field study on the behavior of a foundation underpinned by micropiles. Can Geotech J 43(1):30–42. https://doi.org/10.1139/t05-087

31. Pars Design and Testing Consulting Engineers Company () Final and supplementary report of geotechnical studies of Al-Zahra Hotel

32. ABAQUS (2014) Version 6.14 documentation. Dassault Systemes Simulia Corporation 651, no. 6.2

33. American Association of State Highway and Transportation Officials (AASHTO) (2014) AASHTO LRFD bridge design specifications, 7th edn.

34. Sabatini PJ, Tanyu B, Armour T, Groneck P, Keeley J (2005) Micropile design and construction (reference manual for NHI Course 132078), report no. FHWA-NHI-05-039, National Highway Institute. Federal Highway Administration (FHWA), U.S.A. Department of Transportation, Washington, DC, USA

35. Xiang X, Zi-Hang D (2017) Numerical implementation of a modified Mohr–Coulomb model and its application in slope stability analysis. J Mod Transp 25(1):40–51. https://doi.org/10.1007/s40534-017-0123-0